PERGAMON

Pattern Recognition 36 (2003) 1661 – 1673

PATTERN RECOGNITION
THE JOURNAL OF THE PATTERN RECOGNITION SOCIETY

www.elsevier.com/locate/patcog

A hybrid fingerprint matcher

Arun Ross[a,*], Anil Jain[a], James Reisman[b]

[a] *Department of Computer Science and Engineering, Michigan State University, East Lansing, MI 48824, USA*
[b] *Siemens Corporate Research, Inc., 755 College Road East, Princeton, NJ 08540, USA*

Received 2 November 2001; received in revised form 19 November 2002; accepted 19 November 2002

Abstract

Most fingerprint matching systems rely on the distribution of minutiae on the fingertip to represent and match fingerprints. While the ridge flow pattern is generally used for classifying fingerprints, it is seldom used for matching. This paper describes a hybrid fingerprint matching scheme that uses both minutiae and ridge flow information to represent and match fingerprints. A set of 8 Gabor filters, whose spatial frequencies correspond to the average inter-ridge spacing in fingerprints, is used to capture the ridge strength at equally spaced orientations. A square tessellation of the filtered images is then used to construct an eight-dimensional feature map, called the ridge feature map. The ridge feature map along with the minutiae set of a fingerprint image is used for matching purposes. The proposed technique has the following features: (i) the entire image is taken into account while constructing the ridge feature map; (ii) minutiae matching is used to determine the translation and rotation parameters relating the query and the template images for ridge feature map extraction; (iii) filtering and ridge feature map extraction are implemented in the frequency domain thereby speeding up the matching process; (iv) filtered query images are catched to greatly increase the one-to-many matching speed. The hybrid matcher performs better than a minutiae-based fingerprint matching system. The genuine accept rate of the hybrid matcher is observed to be ∼10% higher than that of a minutiae-based system at low FAR values. Fingerprint verification (one-to-one matching) using the hybrid matcher on a Pentium III, 800 MHz system takes ∼1.4 s, while fingerprint identification (one-to-many matching) involving 1000 templates takes ∼0.2 s per match.

Keywords: Fingerprints; Verification; Identification; Fourier transform; Texture; Ridge flow; Gabor filter

1. Introduction

Among all the biometric indicators [1], fingerprints have one of the highest levels of reliability [2] and have been extensively used by forensic experts in criminal investigations [3]. Although not scientifically established, fingerprints are believed to be unique across individuals, and across fingers of the same individual [4]. Even identical twins having similar DNA, are believed to have different fingerprints. These observations have led to the increased use of *automatic* fingerprint-based identification systems in both civilian and law-enforcement applications.

The uniqueness of a fingerprint is determined by the topographic relief of its ridge structure and the presence of certain ridge anomalies termed as minutiae points (Fig. 1). Typically, the global configuration defined by the ridge structure is used to determine the class [5,6] of the fingerprint, while the distribution of minutiae points is used to match and establish the similarity between two fingerprints [7,8]. Automatic fingerprint identification systems, that match a query print against a large database of prints (which can consist of millions of prints), rely on the pattern of ridges in the query image to narrow their search in the database (*fingerprint indexing*), and on the minutiae points to

* Corresponding author. Tel.: +1-517-355-9319; fax: +1-517-432-1061.

E-mail addresses: rossarun@cse.msu.edu (A. Ross), jain@cse.msu.edu (A. Jain), james.reisman@scr.siemens.com (J. Reisman).

0031-3203/03/$30.00 © 2003 Published by Elsevier Science Ltd on behalf of Pattern Recognition Society.
doi:10.1016/S0031-3203(02)00349-7

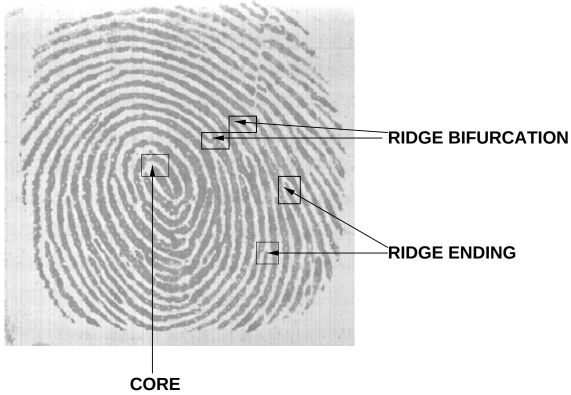

Fig. 1. A fingerprint image with the core and four minutiae points marked on it. The global configuration is defined by the ridge pattern.

determine an exact match (*fingerprint matching*). The ridge flow pattern is seldom used for matching fingerprints.

The ridge pattern in a fingerprint may be viewed as an oriented texture pattern having a fixed dominant spatial frequency and orientation in a local neighborhood. The frequency is due to the inter-ridge spacing present in the fingerprint (Fig. 2(a)), and the orientation is due to the flow pattern exhibited by the ridges (Fig. 2(b)). By capturing the frequency and orientation of ridges in non-overlapping local regions in the fingerprint, a distinct representation of the fingerprint is possible. One such representation has been discussed in [9]. However, to match two fingerprints using such a representation, a suitable alignment of the underlying ridge structures is essential.

We present a fingerprint representation scheme, that constructs a feature map by observing the local ridge orientation in a fingerprint image. The local ridge characteristics are extracted via a set of Gabor filters that are pre-tuned to a specific frequency corresponding to the average inter-ridge spacing in a fingerprint image. An input fingerprint image is filtered using this set of Gabor filters; a square tessellation [10] is then applied to each filtered image to examine the local response to the filter; a feature vector which measures the energy in the filtered images for each of the tessellated cells is next obtained. A collection of these feature vectors (over the tessellation) constitutes the ridge feature map used to represent a fingerprint. Fingerprint matching entails determining the similarity between two such ridge feature maps. This representation is used along with the minutiae set of the fingerprint image for matching purposes. The proposed representation and matching scheme are motivated by the following observations:

(1) Global image information, as defined by the ridge pattern of the fingerprint, is not being explicitly used during the matching phase in most of the current matching systems. We believe that the ridge pattern, when observed at various resolutions and orientations, provides discriminatory information that can be used for matching fingerprints.
(2) Minutiae information may not be very discriminative in the case of solid-state sensors which typically capture only a small area of the fingertip. For example, the average number of minutiae points extracted from Digital Biometrics optical sensor images (500×500 image at 500 dpi) is 45 compared to 25 minutiae obtained from Veridicom solid-state sensor images (300×300 image at 500 dpi). Alternate representations, to supplement minutiae information, are necessary to maintain sufficient fingerprint identification performance in such cases. Further, in poor quality images, while it is difficult to accurately locate minutiae points, the ridge pattern features may be easier to detect.
(3) The problem of aligning and registering fingerprint image pairs is a computationally intensive task. Hybrid matchers, that use minutiae sets to align ridge feature maps, do not require additional computation time for registering images.

In summary, we represent a fingerprint image by a combination of ridge strengths at various orientations, and a set of minutiae points. In the following sections we describe the proposed technique in detail. In Section 2 the problem of fingerprint matching, and the advantages of the proposed technique are presented. Section 3 describes the process of filtering fingerprint images in the frequency domain. Section 4 explains the construction of ridge feature maps via tessellation. Section 5 outlines the minutiae detection algorithm.

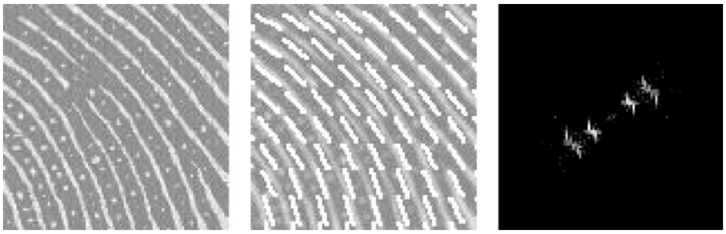

(a) (b) (c)

Fig. 2. Fingerprint as an oriented texture pattern: (a) the constant inter-ridge spacing in a local region of the fingerprint; (b) the dominant direction of the ridges in (a); and (c) the power spectrum of (a).

Section 6 describes the matching process using the hybrid scheme. Section 7 describes the experiments conducted to evaluate the performance of the proposed technique. Section 8 summarizes the paper and presents direction for future work.

2. Fingerprint matching

Fingerprint matching techniques can be broadly classified as being minutiae- or correlation-based. Minutiae-based techniques attempt to align two sets of minutiae points and determine the total number of matched minutiae [11,12,7]. Correlation-based techniques, on the other hand, compare the global pattern of ridges and furrows to see if the ridges in the two fingerprints align [13,14]. The performance of minutiae-based techniques rely on the accurate detection of minutiae points and the use of sophisticated matching techniques to compare two minutiae fields which undergo non-rigid transformations. The performance of correlation-based techniques is affected by non-linear distortions and noise present in the image. In general, it has been observed that minutiae-based techniques perform better than correlation-based ones.

Jain et al. [9] have proposed a novel representation scheme that captures global and local features of a fingerprint in a compact fixed length feature vector termed as *FingerCode*. This technique makes use of the texture features available in a fingerprint to compute the feature vector. Their scheme for generic representation of oriented texture relies on extracting a core point in the fingerprint. A circular region around the core point is located and tessellated into sectors as shown in Fig. 3(a). The pixel intensities in each sector are normalized to a constant mean and variance, and filtered using a bank of eight Gabor filters to produce a set of eight filtered images. Gray scale variance within a sector quantifies the underlying ridge structures and is used as a feature. The feature vector (640 values in length) is the collection of all the features, computed from all the 80 sectors, in every filtered image. The FingerCode captures the *local* information, and the ordered enumeration of the tessellation captures the invariant *global* relationships among the local patterns. The matching stage simply computes the Euclidean distance between the two corresponding FingerCodes. This technique,

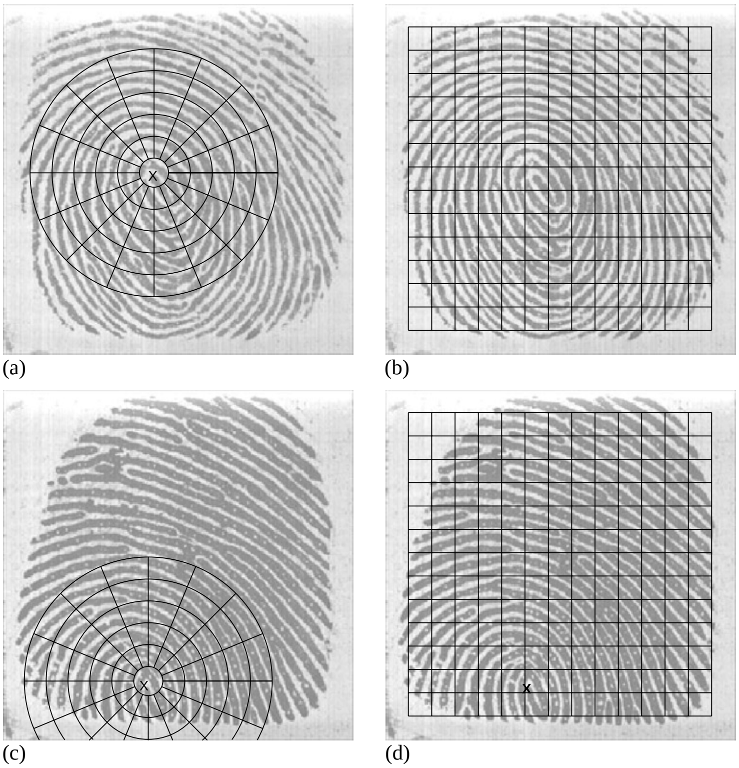

Fig. 3. Tessellating the fingerprint image using a circular and a square grid. The square tessellation, unlike the circular one, is not affected by the location of the core point in the image: (a) circular tessellation about a core point; (b) square tessellation over the entire image; (c) circular tessellation about a core detected close to the boundary of the image; and (d) square tessellation over image in which the core has been detected close to the boundary of the image. The images were acquired using the Veridicom sensor.

however, suffers from the following shortcomings:

(1) The frame of reference is based on a global singular point (i.e., the core point). Detection of the core point is non-trivial; furthermore, the core point may not even be present in small-sized images obtained using solid-state sensors.
(2) The alignment is based on a single reference point and is, therefore, not very robust with respect to errors in the location of the reference point.
(3) The tessellation does not cover the entire image. Furthermore, if the core were to be detected close to the boundary of the image, the tessellation will include an extremely small portion of the image (Fig. 3(c)).

The technique proposed here has the following advantages:

(1) Unlike in Ref. [9], the filtering is done on the enhanced images rather than the raw input images. The enhanced images have lower noise content than the raw images.
(2) Instead of using circular tessellation, a square tessellation is used (Fig. 3(b)). The tessellation includes the entire image, and all the tessellated cells are of the same size. Moreover, the tessellation is not based on detecting any landmark points.
(3) The fingerprint images are aligned using the overall minutiae information; this is more robust than using only the core point for aligning image pairs.

3. Image filtering using Gabor filters

A 2D Gabor filter can be thought of as a complex plane wave modulated by a 2D Gaussian envelope. These filters optimally capture both local orientation and frequency information [1] and their development was motivated by observing the linear response of the receptive field in simple striate cortex cells. By tuning a Gabor filter to a specific frequency and direction, the local frequency and orientation information can be obtained. Thus, they are suited for extracting texture information from images. Daugman has successfully used these filters to extract discriminatory features from the human iris [17].

An even symmetric Gabor filter has the following general form in the spatial domain:

$$G_{\theta,f}(x,y) = \exp\left\{\frac{-1}{2}\left[\frac{x'^2}{\delta_x^2} + \frac{y'^2}{\delta_y^2}\right]\right\}\cos(2\pi f x'),$$

$$x' = x\sin\theta + y\cos\theta,$$

$$y' = x\cos\theta - y\sin\theta, \tag{1}$$

where f is the frequency of the sinusoidal plane wave at an angle θ with the x-axis, and δ_x and δ_y are the standard deviations of the Gaussian envelope along the x- and y-axes, respectively.

For extracting the response of the ridge at various orientations of the Gabor filter, the parameters $(f, \delta_x, \delta_y, \theta)$ are set to the following values:

(i) The frequency, f, corresponds to the inter-ridge distance in fingerprint images. For the 300×300 (500 dpi) images obtained using the Veridicom sensor and resized to 256×256 (see Section 7), the average inter-ridge spacing is about 8 pixels. Hence, $f = \frac{1}{8} = 0.125$.

(ii) The selection of the standard deviation values, δ_x and δ_y, involves a trade-off. Larger values are more robust to noise, but will not capture ridge information at a fine level. Smaller values, on the other hand, are less robust to noise in the image, but capture ridge information very well. Based on empirical data [18], both these values were set to 4, i.e., $\delta_x = \delta_y = \delta = 4$.

(iii) Eight different orientations are examined. These correspond to θ values of $0°, 22.5°, 45°, 67.5°, 90°, 112.5°, 135°, 157.5°$ (Fig. 4).

These parameters are fixed during the matching process, allowing for pre-storing the Gabor filter representations in a lookup table referred to as the Gabor filter bank. This filter bank precalculates the Fourier representation of the Gabor filter for all orientations of interest. This formulation substantially improves the matching time in a one-to-many matching scheme.

3.1. Fingerprint enhancement

Enhancement is the process by which the clarity of the ridge and furrow structures in the fingerprint images is improved to facilitate the feature extraction process [18,19]. Fingerprint enhancement helps in reducing the noise content in the fingerprint image. Enhancement, however, can introduce false ridges, resulting in spurious or missing minutiae points. Since the ridge feature map representation proposed here relies on the *dominant* ridge directions in each tessellated cell, the introduction of false ridges is not a serious problem. The minutiae features are also extracted after processing the enhanced fingerprint image. The enhancement algorithm is based on the technique described in Ref. [18]. Fig. 5 shows a fingerprint image before and after enhancement.

3.2. Fingerprint segmentation

The ridge feature map is constructed using the feature values computed at each tessellated cell. Certain cells may predominantly contain background information, and therefore, the feature values computed at these cells will not be an accurate indication of ridge strength. Thus, the purpose of segmentation is to separate the foreground and background regions in a given fingerprint image. The foreground corresponds to those regions in the image that have

[1] They are optimal in the sense that they try to minimize simultaneously the joint space-spatial frequency uncertainty [15,16].

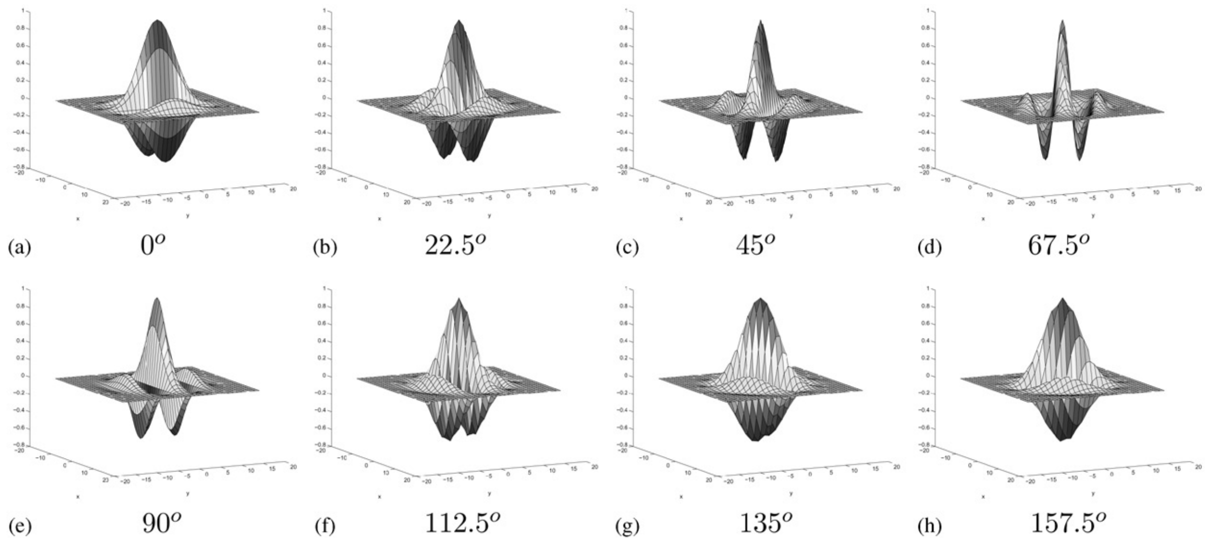

Fig. 4. Gabor filters in spatial domain with eight different orientations used for feature extraction. $f = 0.125, \delta_x = \delta_y = \delta = 4$.

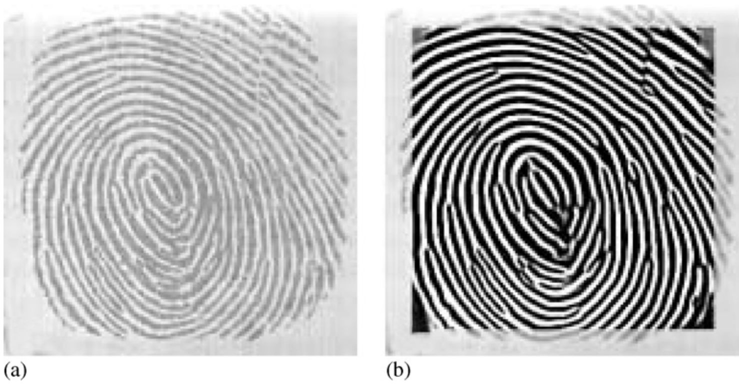

Fig. 5. Fingerprint image: (a) before and (b) after enhancement.

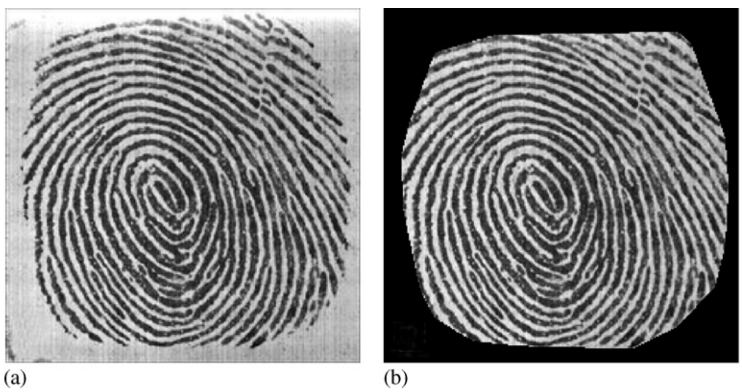

Fig. 6. Segmenting a fingerprint image: (a) the original fingerprint image and (b) the segmented fingerprint image.

relevant fingerprint information (i.e., the ridges and valleys of the fingerprint), while the background represents those regions that do not have the relevant information. Cells with predominantly background information are not used during the matching stage. Segmentation is done by observing the local variation of intensity on the original gray-scale image [7]. Fig. 6 shows a fingerprint image before and after segmentation.

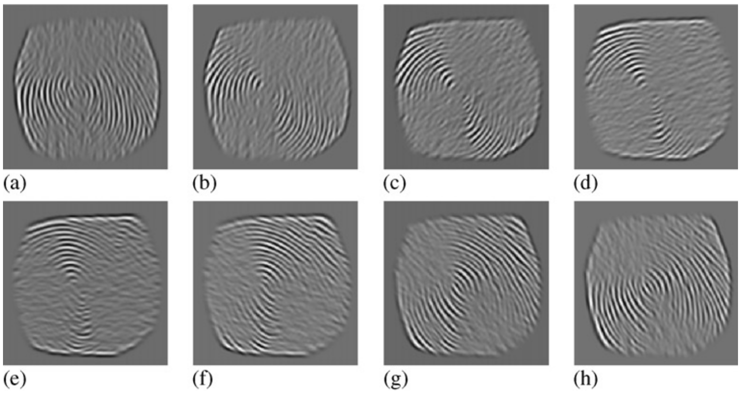

Fig. 7. Results of the filtering process on the image shown in Fig. 5(b). The eight images correspond to the eight different orientations of the Gabor filter.

3.3. Filtering enhanced image

Filtering requires convolving the enhanced image, H, with each of the 8 Gabor filters in the spatial domain. However, such a process would be extremely slow. For a 256×256 image that is convolved with a 16×16 filter, this would mean $\sim 10^7$ multiplications (assuming that the convolution operation has not been optimized). In order to speed-up this operation, the convolution is performed in the frequency domain. Let $\mathscr{F}(H)$ denote the discrete Fourier transform of H, and let $\mathscr{F}(G_\theta)$ indicate the discrete Fourier transform of the Gabor filter having the spatial orientation θ as described by Eq. (1). Thus, the Gabor filtered image, V_θ, may be obtained as

$$V_\theta = \mathscr{F}^{-1}[\mathscr{F}(H)\mathscr{F}(G_\theta)], \tag{2}$$

where $\mathscr{F}^{-1}$ is the inverse Fourier transform. Eight filtered images are obtained as a result of this filtering (Fig. 7).

4. Ridge feature maps

4.1. Tessellation of filtered images

While a filtered image in its entirety can be used as a representation scheme, the presence of local distortions would affect the matching process drastically. Moreover, it is the local variations in ridge structure (combined with the global ridge configuration) that provide a better representation of the fingerprint. To examine local variations, the image is tessellated into square cells, and features from each of the cells are computed (Fig. 8). The size of a cell is chosen to correspond to approximately the width of two ridges (16×16). A 8 pixel wide border of the image is not included in the tessellation. This results in $n_c = 15$ cells in each row and column of the square grid. The total number of tessellated cells over the image is, therefore, $N_c = 225$. The *variance* of the pixel intensities in each cell across all filtered images is used as a feature vector. The variance corresponds to the energy of the filter response, and is, therefore, a useful measure of ridge orientation in a local neighborhood. Those tessellated cells that contain a certain proportion of background pixels are labeled as background cells and the corresponding feature value is set to 0.

4.2. Ridge feature map definition

Let $C_\theta(i,j)$ refer to the (i,j)th cell in the square grid that is placed on the filtered image V_θ. The variance, $\sigma_\theta^2(i,j)$, represents the feature value corresponding to the cell. Thus, for each V_θ, a feature map of variance values can be obtained. Let R_θ denote the feature map associated with the filtered

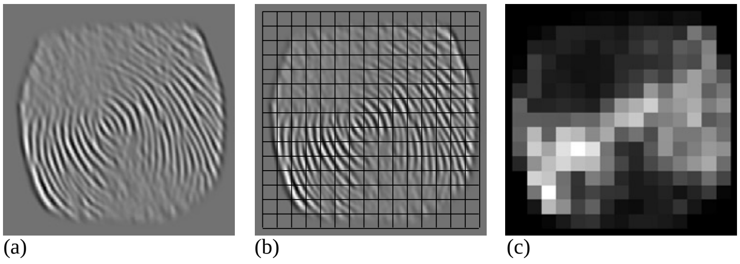

Fig. 8. Tessellating the filtered image: (a) a fingerprint image filtered with a Gabor filter oriented at 157.5°; (b) a square tessellation of the filtered image; and (c) the ridge feature map ($n_c \times n_c$) representation of the fingerprint.

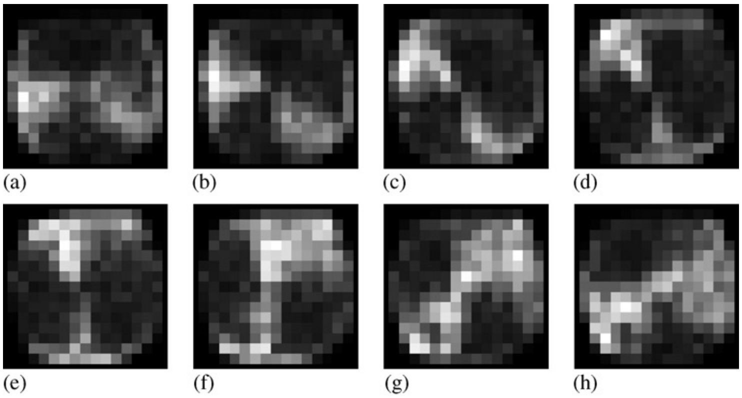

Fig. 9. Feature maps representing the variance in intensity in the filtered images for each cell. For purposes of visualization, the feature values have been scaled to the 0–255 range.

image V_θ. Then,

$$R_\theta = \{\sigma_\theta^2(i,j)\}, \tag{3}$$

where, $\theta \in \{0°, 22.5°, 45°, 67.5°, 90°, 112.5°, 135°, 157.5°\}$, $i = 1, \ldots, n_c,\ j = 1, \ldots, n_c$.

An eight-dimensional feature map corresponding to the eight filtered images is obtained in this way (Fig. 9). These ridge feature maps are used to represent and match a query image with a template.

5. Minutiae extraction

Minutiae extraction refers to the process by which the minutiae points are detected in a fingerprint image. Each minutiae is characterized by its (x, y) location in the image, and the orientation θ of the ridge on which it is detected. The ridge information in a 64×64 region around the (x, y) point is associated with every minutiae which is useful when two minutiae sets are being matched. The minutiae extraction scheme (Fig. 10) can be broadly classified into the following stages:

(i) *Orientation field estimation*: The orientation of the fingerprint image is computed in non-overlapping blocks by examining the gradients of pixel intensities in the x and y directions within the block.

(ii) *Ridge detection*: The ridges present in the fingerprint image are identified by applying masks that are capable of accentuating the local maximum gray level values along the normal direction of the local ridge direction.

(iii) *Ridge thinning*: The ridge map constructed in the earlier stage is used to obtain a thinned ridge image.

(iv) *Minutiae detection*: A set of rules is applied to the thinned ridges to label minutiae points (ridge endings and ridge bifurcations). As a postprocessing step, a refinement algorithm is applied to remove spurious minutiae points.

Minutiae matching involves a point matching operation on the two minutiae sets. An elastic string matching technique is employed to compare the two minutiae sets [7]. The output of the matching process is a matching score that indicates the similarity of the two sets being compared, and a correspondence map that indicates pairing of minutiae points from the two sets. The correspondence map is used to compute the transformation parameters necessary to align the two fingerprint images.

6. Hybrid fingerprint matcher

The process of fingerprint matching involves comparing a query print with a set of one or more template prints. Prior to the matching process, feature information is extracted from all the template images (Fig. 11). The hybrid fingerprint matcher proposed here utilizes two distinct sets of fingerprint information for matching fingerprints: minutiae features, and ridge feature maps. When a query image is presented, the matching proceeds as follows: (i) the query and template minutiae features are matched to generate a minutiae matching score and a transformation parameter (translation and rotation) that relates the query and template fingerprints; (ii) the rotation parameter is used to rotate the 8 Gabor filters and the modified filters are applied to the query image; (iii) the filtered query images are then translated and rotated according to the parameters; (iv) the ridge feature map is extracted from these filtered images; (v) the query and template ridge feature maps are matched; (vi) the minutiae and ridge feature map matching results are combined to generate a single matching score (Fig. 12).

6.1. Aligning query and template images

For comparing the ridge feature maps of two images, it is necessary that the images themselves are aligned appropriately to ensure an overlap of common region in the two fingerprint images. This is done by determining the

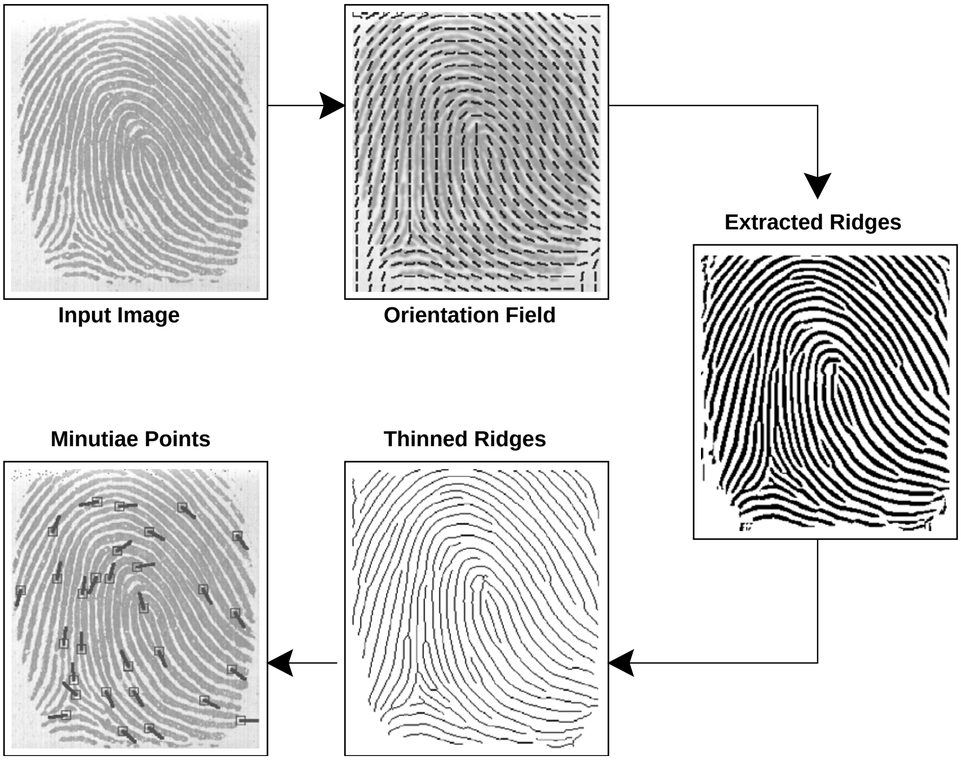

Fig. 10. Flowchart of the minutiae extraction algorithm [7].

transformation parameters, (t_x, t_y, t_ϕ), that would align the query image with the template. As indicated in Section 5, the correspondence map provided by the minutiae matcher is used to compute (t_x, t_y, t_ϕ).

Once the transformation parameters, (t_x, t_y, t_ϕ), are obtained, the query image can be aligned with the template. But rotating the query image will result in artifacts that may affect the subsequent filtering operation. In order to avoid this, appropriately rotated Gabor filters (which are also stored in the Gabor filter bank) are applied to the query image. The resulting *filtered images* are then rotated and feature values extracted. Let H represent the enhanced query image, and (t_x, t_y, t_ϕ) be the translation and rotation parameters obtained using the minutiae matching information. Then the filtered image, V_{θ,t_ϕ}, is obtained as

$$V_{\theta,t_\phi} = Rot_{t_\phi}\mathscr{F}^{-1}[\mathscr{F}(H)\mathscr{F}(G_{\theta-t_\phi})], \tag{4}$$

where Rot_{t_ϕ} indicates that the filtered image is rotated by an angle t_ϕ. The notation V_{θ,t_ϕ} is used to indicate that the filtered image corresponding to filter orientation $\theta - t_\phi$ was rotated through an angle t_ϕ. The filtered image is then translated by (t_x, t_y), in order to ensure that the tessellation of the query image would overlap with that of the template.

6.2. Matching scores

The minutiae matching score is a measure of the similarity of the minutiae sets of the query and template images; the higher the matching score the better the match. The similarity score is normalized in the $[0, 100]$ range. The ridge feature maps of the query and the template images are compared by computing the sum of the Euclidean distances of the eight-dimensional feature vectors in the corresponding tessellated cells. Cells that are marked as background, are not used in the matching process. This results in a *distance* score measure; a higher distance score indicates a poor match. The distance score is normalized in the $[0, 100]$ range, and converted to a similarity score by simply subtracting it from 100.

6.3. Combining matching scores

The matching scores generated by comparing the minutiae sets and the ridge feature maps, are combined in order to generate a single matching score. While a variety of strategies [20] may be used to fuse these scores, we adopt the following sum rule. Let S_M and S_R indicate the similarity scores obtained using minutiae matching and ridge feature map matching, respectively. Then, the final matching score,

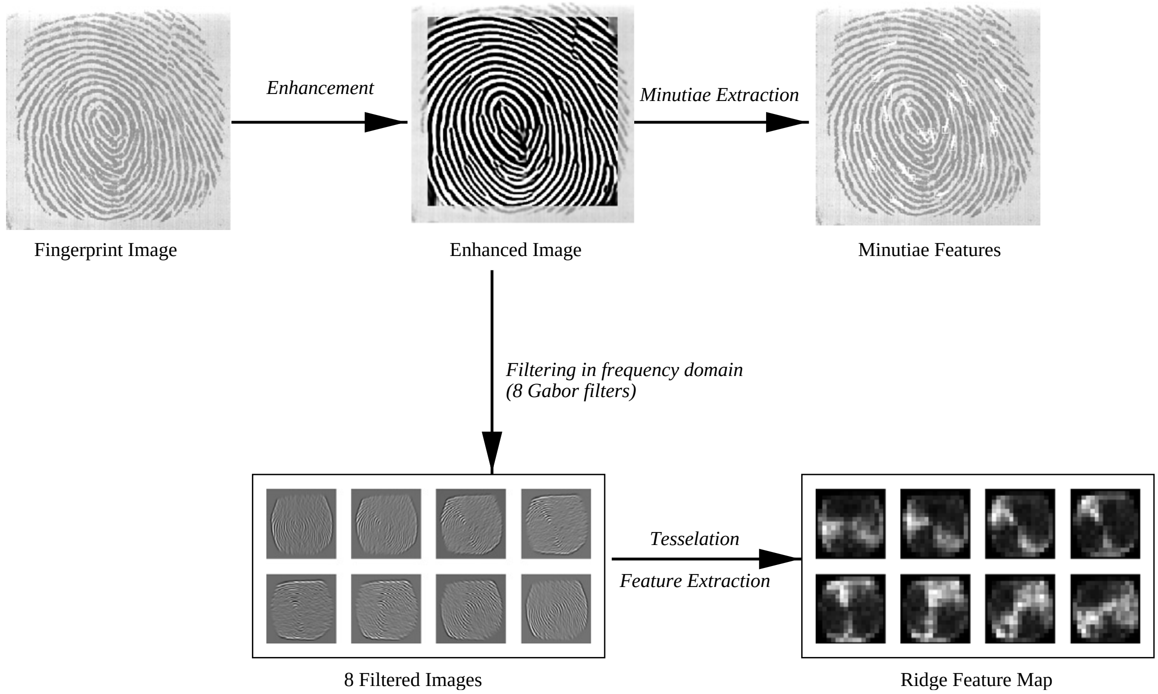

Fig. 11. Template feature extraction. A minutiae set and a ridge feature map are extracted from the input fingerprint image.

S, is computed as

$$S = \alpha S_M + (1 - \alpha) S_R, \tag{5}$$

where $\alpha \in [0, 1]$. For the experimental results reported in this paper, α was set to 0.5. It is possible to vary α to assign different weights to the individual matchers.

6.4. Fingerprint identification

Fingerprint identification involves matching a query image against *multiple* templates (corresponding to different users) in order to determine the best matching score and, therefore, the template that best resembles it. It is obvious that the processing time required to perform identification (one-to-many matching) is substantially more than that required for verification (one-to-one matching). In order to reduce the number of matching operations, most fingerprint identification systems use some indexing mechanism, to narrow the number of templates against which the query image has to be matched. A variety of fingerprint indexing mechanisms have been proposed in the literature [5,21–23]. However, in the identification process described in this paper, we do not use an indexing mechanism to limit the number of matchings. The identification process requires filtering and rotating the query image for every match that is performed (Eq. (4)). Computing V_{θ,t_ϕ} is an expensive operation because of the Fourier operations performed. To decrease the computational complexity involved, a combination of frequency domain filtering, and filtered image-caching, is done. Caching V_{θ,t_ϕ} avoids recomputing this filtered image. Each time a query image, Q, is presented, the following sequence of operations is performed:

Step 1: Let the image-cache be represented by K. Set $K = \Phi$ (the empty set).

Step 2: Extract the minutiae set of Q, M^Q.

For all the templates $\{T_i\}$ in the database, represented by their minutiae set $\{M^{T_i}\}$ and ridge feature map $\{R^{T_i}\}$, do Steps 3–7.

Step 3: Compute the transformation parameters, (t_x, t_y, t_ϕ), relating Q and T_i, using the minutiae sets M^Q and M^{T_i} as described earlier.

Step 4: If $V_{\theta,t_\phi} \in K$, do Step 6.

Step 5: Compute V_{θ,t_ϕ} according to Eq. (4). $K = K \cup V_{\theta,t_\phi}$.

Step 6: Offset V_{θ,t_ϕ} using (t_x, t_y) and perform tessellation and ridge feature map extraction. Let R^Q be the ridge feature map of the query image.

Step 7: Use M^Q, M^{T_i}, R^Q and R^{T_i} to generate the matching scores S_{M_i} and S_{R_i}. Combine scores using Eq. (5) to obtain a single matching score S_i.

Step 8: The template T_j that results in the highest matching score ($S_j > S_k \ \forall j \neq k$) is reported as the closest match to the query image Q.

Step 5 is performed only when V_{θ,t_ϕ} has *not* been computed at an earlier stage, thus improving the speed of the one-to-many matching process.

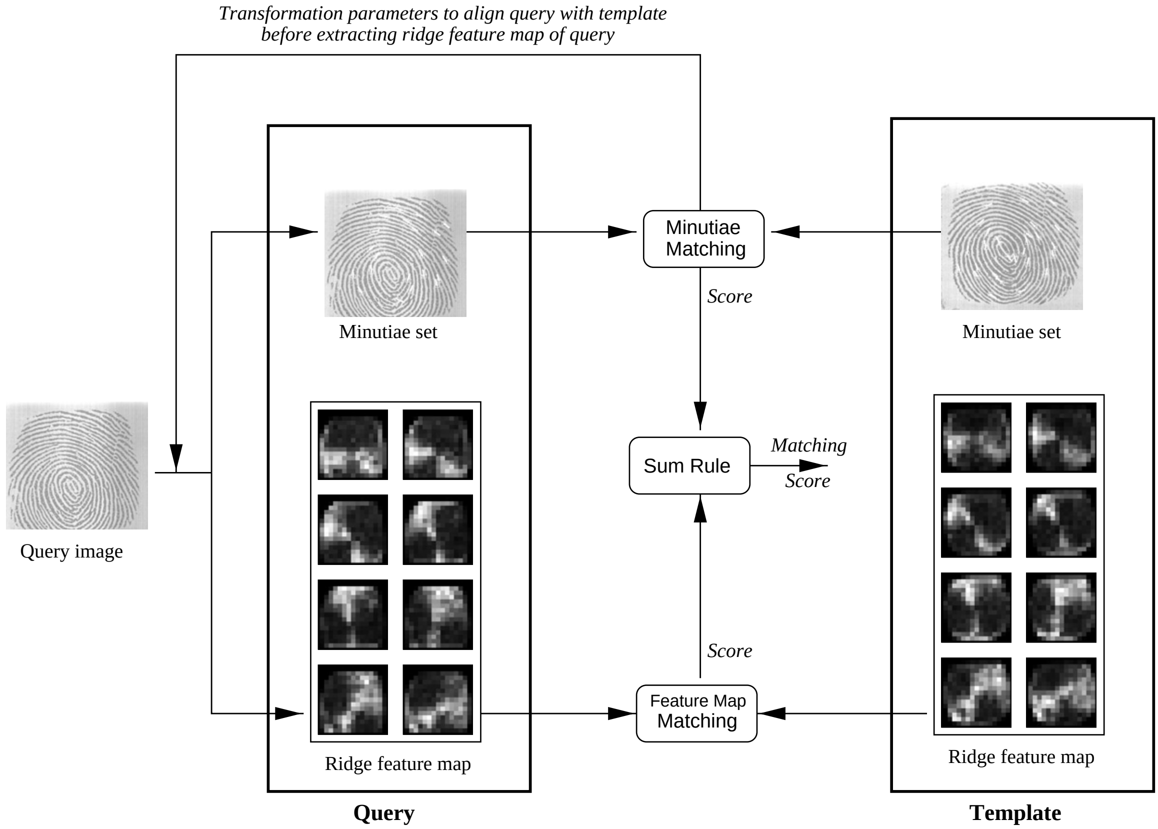

Fig. 12. The matching process. The minutiae matching module provides the transformation parameters necessary to align the query image with the template.

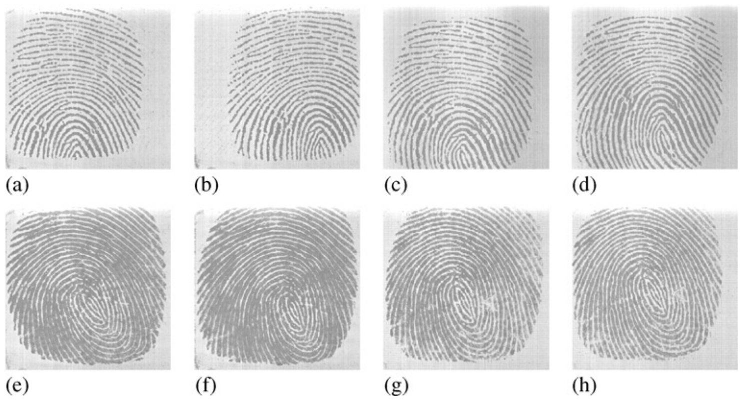

Fig. 13. Eight 300 × 300 fingerprint impressions acquired using the Veridicom sensor. Images (a)–(d) correspond to the right index finger of one subject, and images (e) and (h) correspond to the right middle finger of another subject. The images are resized to 256 × 256 to speed-up Fourier operations.

7. Experiments and results

The fingerprint database used in our experiments consists of fingerprint impressions obtained from 160 non-habituated, cooperative subjects using the Veridicom sensor (300 × 300 images at 500 dpi). The data was collected over two sessions. The subjects mainly consisted of students, faculty and staff at Michigan State University, and their relatives and friends. Approximately 35% of the subjects were women. In the first session, each subject was asked to provide two impressions of each of four different fingers—the left index finger, the left middle finger, the

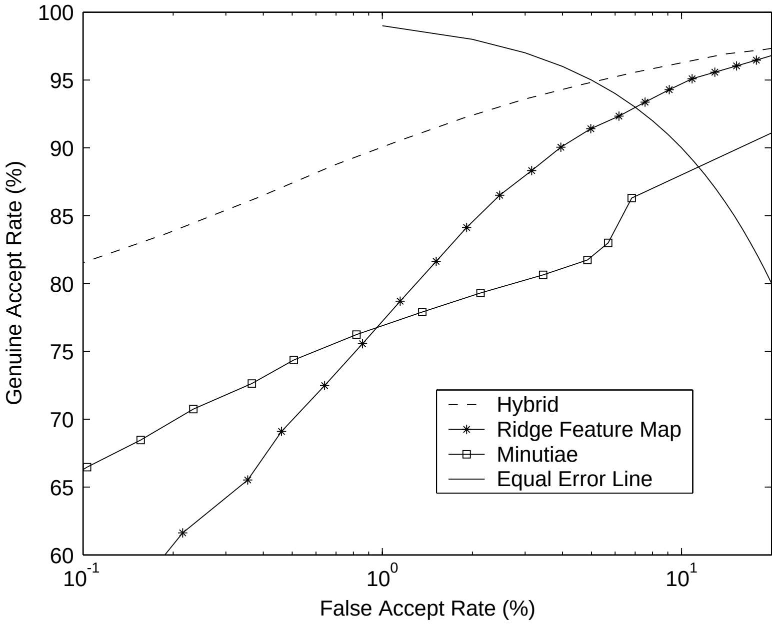

Fig. 14. ROC showing the performances of the three matchers. The hybrid matcher is observed to perform better than the minutiae matcher.

(a) (b)

Fig. 15. Two impressions of the same finger that have a high minutiae matching score but a low ridge feature map matching score. The hybrid score results in a true match.

right index finger and the right middle finger. A set of 1280 ($160 \times 4 \times 2$) images were collected in this way. The subjects were requested to provide their fingerprint images again, after a period of 6 weeks. During the second session, the same procedure was adopted, and an additional 1280 images were obtained. Thus, a total of 2560 images were acquired over two time sessions (Fig. 13). The 300×300 images were resized to 256×256 [2] in order to speed-up the Fourier operations. The average inter-ridge distance was computed using 640 images (one impression per finger).

The performance of a biometric system can be measured by reporting its false accept rate (FAR) and false reject rate (FRR) at various thresholds. These two error rates are brought together in a receiver operating characteristic (ROC) curve that plots the FRR against the FAR at different thresholds. (Alternately, the genuine accept rate (GAR), which equals 1-FRR, may be plotted against the FAR.) The FAR and FRR are computed by generating all possible genuine and impostor matching scores and then setting a threshold for deciding whether to accept or reject a match. A genuine matching score is obtained when two feature vectors corresponding to the *same* individual are

[2] The images were first resized to 240×240 using a bicubic interpolation; they were then padded with zeros to increase the size to 256×256. This was necessary to avoid the wrap-around distortions at the border when the image is convolved with the Gabor filter.

(a) (b)

Fig. 16. Two impressions of the same finger that have a low minutiae matching score but a high ridge feature map matching score. The hybrid score results in a true match.

compared, and an impostor matching score is obtained when feature vectors from two *different* individuals are compared.

The ROC curves depicting the performances of the minutiae, ridge feature map and hybrid matchers are shown in Fig. 14. The hybrid technique outperforms the minutiae-based scheme over a wide range of FAR values. For example, at a FAR of 0.1%, the GAR of the minutiae matcher is ∼67%, while that of the hybrid matcher is ∼84%. The equal error rate of the hybrid technique is observed to be ∼4%. The experiments also show that the minutiae information and ridge flow information complement each other. Consider Fig. 15 that shows two different impressions of a finger. For this pair, matching the minutiae sets results in a high matching score, but matching the ridge feature map results in a low score (due to the limited amount of foreground overlap between the two impressions). The hybrid score, however, results in a positive match (at a certain matching threshold) between the two impressions. Now consider the fingerprint impressions (of another finger) in Fig. 16. The minutiae matching score is rather low in this case (due to spurious minutiae being detected in both images), while the ridge feature map matching score is high (enhancing the image provides sharp dominant ridge directions). The hybrid score results in a positive match of the two impressions (at a certain matching threshold), thereby underlining the importance of the proposed technique.

The experiments reported here were conducted on a Pentium III, 800 MHz processor, running Windows 2000. Minutiae extraction took ∼1 s, while ridge feature map computation took ∼0.3 s. The time taken to match two minutiae sets and generate the transformation parameters was ∼0.02 s. Matching two ridge feature maps took ∼0.01 s. The total time for fingerprint verification (one-to-one matching) was ∼1.4 s. However, fingerprint identification (one-to-many matching), involving 1000 templates, took only ∼0.2 s per match (average), because of the filtered image-cache.

8. Summary and future work

In this paper, a novel fingerprint representation technique that uses ridge feature maps has been presented. Further, a hybrid fingerprint matching technique that combines minutiae information with the ridge feature map has been described. Experiments indicate that the hybrid technique performs much better than a purely minutiae-based matching scheme. Currently, minutiae information is being used to align the query and the template images, before computing the ridge feature map of the query image. We are working on non-minutiae based alignment techniques that make use of orientation field and ridge feature map information to align image pairs. The following areas of improvement are also being studied:

(1) New matching methods for comparing the ridge feature maps of two images.
(2) Development of fusion architectures to improve performance of the hybrid matcher.
(3) Constructing the ridge feature maps using adaptive methods for optimal selection of the Gabor filters.

References

[1] A.K. Jain, R. Bolle, S. Pankanti (Eds.), Biometrics: Personal Identification in Networked Society, Kluwer Academic Publishers, Dordrecht, 1999.

[2] J. Berry, D.A. Stoney, The history and development of fingerprinting, in: H.C. Lee, R. Gaensslen (Eds.), Advances in Fingerprint Technology, 2nd Edition, CRC Press, Boca Raton, FL, 2001, pp. 1–40.

[3] Federal Bureau of Investigation, The Science of Fingerprints: Classification and Uses, Government Printing Office, Washington, DC, US, 1984.

[4] S. Pankanti, S. Prabhakar, A.K. Jain, On the individuality of fingerprints, IEEE Trans. Pattern Anal. Mach. Intell. 24 (8) (2002) 1010–1025.

[5] K. Karu, A.K. Jain, Fingerprint classification, Pattern Recognition 29 (3) (1996) 389–404.
[6] A. Senior, A combination fingerprint classifier, IEEE Trans. Pattern Anal. Mach. Intell. 23 (10) (2001) 1165–1174.
[7] A.K. Jain, L. Hong, R. Bolle, On-line fingerprint verification, IEEE Trans. Pattern Anal. Mach. Intell. 19 (4) (1997) 302–314.
[8] Z.M. Kovács-Vajna, A fingerprint verification system based on triangular matching and dynamic time warping, IEEE Trans. Pattern Anal. Mach. Intell. 22 (11) (2000) 1266–1276.
[9] A.K. Jain, S. Prabhakar, L. Hong, S. Pankanti, Filter-bank-based fingerprint matching, IEEE Trans. Image Process. 9 (5) (2000) 846–859.
[10] A.K. Jain, A. Ross, S. Prabhakar, Fingerprint matching using minutiae and texture features, in: Proceedings of the International Conference on Image Processing (ICIP), Thessaloniki, Greece, 2001, pp. 282–285.
[11] F. Pernus, S. Kovacic, L. Gyergyek, Minutiae-based fingerprint recognition, in: Proceedings of the Fifth International Conference on Pattern Recognition, Miami Beach, FL, USA, 1980, pp. 1380–1382.
[12] B. Mehtre, M. Murthy, A minutiae-based fingerprint identification system, in: Proceedings of the Second International Conference on Advances in Pattern Recognition and Digital Techniques, Calcutta, India, 1986.
[13] A. Sibbald, Method and apparatus for fingerprint characterization and recognition using auto-correlation pattern, US Patent 5633947, 1994.
[14] A.M. Bazen, G.T.B. Verwaaijen, S.H. Gerez, L.P.J. Veelenturf, B.J. van der Zwaag, A correlation-based fingerprint verification system, in: Proceedings of the ProRISC2000 Workshop on Circuits, Systems and Signal Processing, Veldhoven, Netherlands, 2000.
[15] J. Daugman, Uncertainty relation for resolution in space, spatial frequency, and orientation optimized by two-dimensional visual cortical filters, J. Opt. Soc. Am. 2 (1985) 1160–1169.
[16] S. Klein, B. Beutter, Minimizing and maximizing the joint space-spatial frequency uncertainty of gabor-like functions: comment, J. Opt. Soc. Am. 9 (2) (1992) 337–340.
[17] J. Daugman, Recognizing persons by their iris patterns, in: A.K. Jain, R. Bolle, S. Pankanti (Eds.), Biometrics: Personal Identification in a Networked Society, Kluwer Academic Publishers, Dordrecht, 1999, pp. 103–121.
[18] L. Hong, Y. Wan, A.K. Jain, Fingerprint image enhancement: Algorithms and performance evaluation, IEEE Trans. Pattern Anal. Mach. Intell. 20 (8) (1998) 777–789.
[19] D. Sherlock, D.M. Monro, K. Millard, Fingerprint enhancement by directional fourier filtering, IEE Proc. Vision, Image Signal Process. 141 (2) (1994) 87–94.
[20] J. Kittler, M. Hatef, R.P. Duin, J.G. Matas, On combining classifiers, IEEE Trans. Pattern Anal. Mach. Intell. 20 (3) (1998) 226–239.
[21] R. Germain, A. Califano, S. Colville, Fingerprint matching using transformation parameters, IEEE Comput. Sci. Eng. 4 (4) (1997) 42–49.
[22] B. Bhanu, X. Tan, A triplet-based approach for indexing of fingerprint database for identification, in: Proceedings of the Third International Conference on Audio and Video-based Biometric Person Authentication (AVBPA), Halmstad, Sweden, 2001, pp. 205–210.
[23] R. Cappelli, D. Maio, D. Maltoni, Fingerprint classification by directional image partitioning, IEEE Trans. Pattern Anal. Mach. Intell. 21 (5) (1999) 402–421.

About the Author—ARUN ROSS obtained the M.S. degree in Computer Science and Engineering from Michigan State University, USA in 1999, and the B.E. (Hons.) degree in Computer Science from the Birla Institute of Technology and Science, Pilani, India in 1996. He is currently a Ph.D. student at Michigan State University and his dissertation research is on integrating information in fingerprint authentication. His areas of interest are statistical pattern recognition, machine learning, data-mining and biometric authentication.

About the Author—ANIL JAIN is a University Distinguished Professor in the Department of Computer Science and Engineering at Michigan State University. He has made significant contributions and published a large number of papers on the following topics: statistical pattern recognition, exploratory pattern analysis, neural networks, Markov random fields, texture analysis, interpretation of range images, 3D object recognition, document image analysis and biometric authentication. He is a fellow of the IEEE and International Association of Pattern Recognition (IAPR). He received a Fulbright Research Award in 1998 and a Guggenheim fellowship in 2001.

About the Author—JAMES REISMAN received his B.Sc. degree in Electrical Engineering from Carnegie Mellon University, and his Ph.D. in Electrical Engineering from Penn State University. He has been a Member of the Technical Staff at Siemens Corporate Research in Princeton, NJ, since 2000. His research interests and current projects include fingerprint recognition and analysis, and medical imaging.